ORIGINAL PAPER

CrossMark

Influences of the substituents on the Cr=C bond in [(OC)$_5$Cr=C(OEt)-*para*-C$_6$H$_4$X] complexes: quantum Theory of Atoms in Molecules, Energy Decomposition Analysis, and Interacting Quantum Atoms
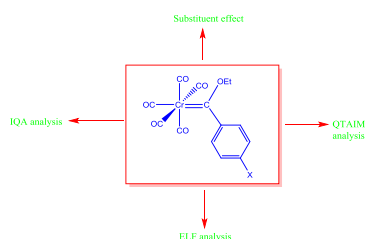
Reza Ghiasi[1] · Sarvin Hossien Saraf[1] · Hoda Pasdar[2]

Abstract

This study was conducted to investigate the effect of various substituents on the Cr=C bond in the [(OC)$_5$Cr=C(OEt)-*para*-C$_6$H$_4$X] complexes using B3LYP*-based quantum mechanical calculations. In this respect, the study evaluates the influence of electron withdrawing and donating groups on the Cr=C bond distances and topological properties and correlates the calculated parameters with the Hammett and Brown constants for the *para*-substituted (σ_P and σ_P^+, respectively) functional groups. Also, the frontier orbital analysis was used to show the electronic structure of complexes and the percentage composition in terms of the defined groups of frontier orbitals was evaluated. To obtain insight into the physical nature of Cr=C bond bonds, we extensively used energy decomposition analysis and Bader's Quantum Theory of Atoms-in-Molecules (QTAIM). With this aim, in addition to examining the bond critical points properties, we apply Pendás' Interacting Quantum Atoms (IQA) scheme, which enables the rigorous and physical study of Cr=C bonds in these complexes.

Graphical abstract

✉ Reza Ghiasi
  rezaghiasi1353@yahoo.com; rghiasi@iauet.ac.ir

[1] Department of Chemistry, East Tehran Branch, Islamic Azad University, Tehran, Iran

[2] Faculty of Chemistry, North Tehran Branch, Islamic Azad University, Tehran, Iran

Introduction

Carbenes are special classes of carbon-containing compounds that are considered as reactive intermediates in various organic transformations because of their incomplete electronic state and coordinative unsaturation. Nowadays, several stable carbenes [1–3] have been isolated and this field is becoming an active area of research. Carbene organometallic complexes have recently received much attention because of the possible involvement of these species in catalytic reactions

[4–7]. Furthermore, these complexes have interesting bonding and reactivity characteristic and play significant roles in synthetic organic and polymer chemistry [8–14]. Many theoretical studies illustrated the structures and different features of these complexes [15–20]. The organometallic photochemistry of chromium(0) carbene complexes is, perhaps, one of the few metal-mediated photoreactions of general application in organic synthesis [21–25]. In this regard, TD-DFT and experimental study of the electronic structure of alkoxychromium(0) carbene complexes have been reported [26].

Many studies have reported the substituent effects on different physical and chemical properties. Quantum chemical investigations can afford useful relationships between the electronic and structural characteristics [27–32]. Accordingly, various computational investigations have reported substituent impact on the structural, electronic, and spectroscopic properties of organometallic complexes [17, 33–44].

Furthermore, quantitative substituent parameter scales have been found useful in clarifying the polar or steric effects of the substituent on molecular properties. For instance, the Hammett constant (σ_p) [45] and Brown constant (σ_p^+) [46] described the electronic effects of substituents on the equilibrium and rate constants of a reacting molecule. It is noteworthy that the Brown's σ_p^+ substituent constant reflects the polar induction/resonance effects of a substituent. Thus, a positive σ_p^+ value means that a substituent is electron-withdrawing; otherwise, it is electron-donating.

In this work, we report a computational study about the effect of substitution on the Cr=C bond in the $[(OC)_5\text{-}Cr=C(OEt)\text{-}para\text{-}C_6H_4X]$ complexes by quantum chemical calculations.

Results and discussion

Structural parameters

Figure 1 presents the structure of the studied $[(OC)_5\text{-}Cr=C(OEt)\text{-}para\text{-}C_6H_4X]$ complexes. The Cr=C$_{carbene}$
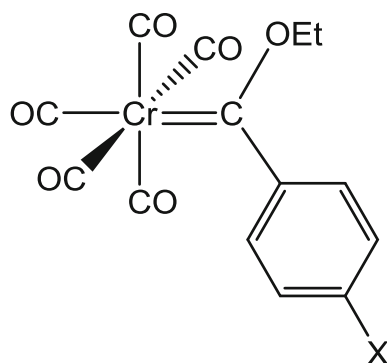

Fig. 1 The structure of the studied $[(OC)_5Cr=C(OEt)\text{-}para\text{-}C_6H_4X]$ complexes

bond distances in these complexes are listed in Table 1. As can be seen, longer bond distances occur in the presence of electron donating groups (EDG). This increase in bond distances is explained with II-resonance form of $[(OC)_5\text{-}Cr=C(OEt)\text{-}para\text{-}C_6H_4X]$ complexes in the presence of EDGs (Fig. 2). The relations between bond distances values with the Hammett (σ_p) and the Brown's (σ_p^+) substituent constants are:

$$r = -0.0363\sigma_p + 2.1147 \quad R^2 = 0.9539,$$
$$r = -0.0241\sigma_p^+ + 2.1098 \quad R^2 = 0.988.$$

Therefore, there is a good correlation between these Cr=C$_{carbene}$ bond distance values and Brown's substituent constant compared to the Hammett constant.

Molecular orbital analysis

The values of frontier orbital energies and their gap are listed in Table 2. According to the calculation results, frontier orbitals are stabilized in the presence of electron withdrawing groups (EWG) and destabilized in the presence of EDGs. The relationships between the frontier orbital energy values with the Hammett (σ_p) and the Brown's (σ_p^+) substituent constants are:

$$E_{HOMO} = -0.405\sigma_p - 5.448 \quad R^2 = 0.9809,$$
$$E_{HOMO} = -0.2564\sigma_p^+ - 5.5033 \quad R^2 = 0.9218,$$
$$E_{LUMO} = -0.6258\sigma_p - 2.4117 \quad R^2 = 0.9258,$$
$$E_{LUMO} = -0.4077\sigma_p^+ - 2.5008 \quad R^2 = 0.8505.$$

As can be noted, there are good correlations between the HOMO energy values and Hammett substituent constants (σ_p) compared to the Brown's (σ_p^+) substituent constants. Also, there is a good correlation between frontier orbital energy, as:

$$E_{HOMO} = 1.6111\, E_{LUMO} + 6.3653 \quad R^2 = 0.9469.$$

This strong correlation is attributed to similar topologies of frontier orbitals in the presence of various substituents. As shown in Table 2, there are larger the HOMO–LUMO gap values in the presence of EDGs compared to EWGs.

Therefore, EWGs have the lowest LUMO energy, resulting in the smallest HOMO–LUMO gap for these studied complexes. This behavior arises from an electron-withdrawing inductive effect, which concentrates the electronic density over the substituted region of the complex. On the contrary, the largest HOMO–LUMO gap was established for EDGs due to the electron donating character of the substituent. These good correlations suggest that EWGs/EDGs influence the frontier orbital energies and the HOMO–LUMO gaps. Therefore, these correlations may be

Table 1 Cr-C bond distance, EDA analysis results in [(OC)$_5$Cr=C(OEt)-*para*-C$_6$H$_4$X] complexes

X	σ_p	σ_p^+	Cr-C/Å	E_{inter}/kJ mol^{-1}	ΔE_{polar}/kJ mol^{-1}	ΔE_{steric}/kJ mol^{-1}
OH	− 0.66	− 0.92	2.1304	− 208.32	− 231.88	23.51
NH$_2$	− 0.37	− 1.30	2.1437	− 210.58	− 228.57	17.99
Me	− 0.17	− 0.31	2.1161	− 209.49	− 237.02	27.53
H	0.00	0.00	2.1090	− 209.07	− 239.49	30.38
Cl	0.23	0.11	2.1067	− 206.40	− 239.66	33.26
CHO	0.42	0.73	2.0962	− 206.61	− 245.02	38.41
COOH	0.45	0.42	2.0980	− 207.28	− 244.05	36.78
CN	0.66	0.66	2.0941	− 204.97	− 245.35	40.38
NO$_2$	0.78	0.79	2.0898	− 204.89	− 247.61	42.72

σ_p and σ_p^+ are Hammett and Brown constants of substituents, respectively
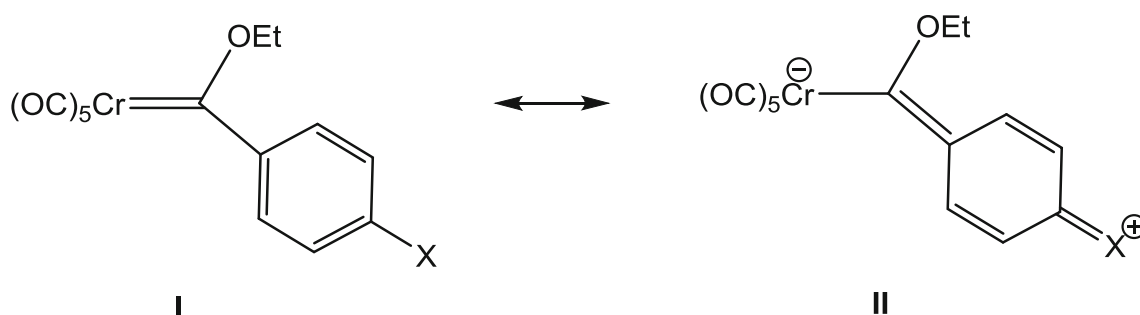
Fig. 2 Resonance forms of [(OC)$_5$Cr=C(OEt)-*para*-C$_6$H$_4$X] complexes in the presence of EDGs

Table 2 Frontier orbital energy values, HOMO–LUMO gap, hardness (η), chemical potential (μ), electrophilicity (ω), electrodonating (ω^-), and electroaccepting (ω^+) powers and net electrophilicity ($\Delta\omega^\pm$) for [(OC)$_5$Cr=C(OEt)-*para*-C$_6$H$_4$X] complexes

X	E_{HOMO}/eV	E_{LUMO}/Ev	Gap/eV	η/eV	μ/eV	ω/eV	ω^+	ω^-	$\Delta\omega^\pm$
OH	− 5.337	− 2.229	3.108	1.554	− 3.783	3.108	5.815	13.382	19.197
NH$_2$	− 5.167	− 2.052	3.114	1.557	− 3.609	3.114	5.146	12.365	17.512
Me	− 5.369	− 2.251	3.118	1.559	− 3.810	3.118	5.890	13.511	19.401
H	− 5.428	− 2.301	3.126	1.563	− 3.864	3.126	6.080	13.809	19.889
Cl	− 5.553	− 2.487	3.066	1.533	− 4.020	3.066	6.903	14.942	21.846
CHO	− 5.644	− 2.784	2.860	1.430	− 4.214	2.860	8.563	16.992	25.555
COOH	− 5.578	− 2.626	2.952	1.476	− 4.102	2.952	7.668	15.872	23.540
CN	− 5.731	− 2.805	2.926	1.463	− 4.268	2.926	8.548	17.084	25.632
NO$_2$	− 5.768	− 3.045	2.723	1.362	− 4.407	2.723	10.197	19.010	29.207

employed to calculate these parameters for other substituents for which σ_p and σ_p^+ are known.

Frontier orbital distributions

The frontier orbital distributions of the [(OC)$_5$Cr=C(OEt)-C$_6$H$_5$] complex are plotted in Fig. 3. It can be seen that there is not any overlapping between atomic orbitals of chromium and C$_{carbene}$ in HOMO. But, there is a π^*-overlap between atomic orbitals of chromium and C$_{carbene}$ in LUMO. The percentage composition in terms of the defined groups of frontier orbitals for [(OC)$_5$Cr=C(OEt)-*para*-C$_6$H$_4$X] complexes was studied to understand the character of the metal–ligand bonds and are listed in

Table 3. These values show that the largest contributions of the HOMO arise from Cr(CO)$_5$ fragment. Moreover, the largest contribution of LUMO arises from the C(OEt)-*para*-C$_6$H$_4$X group.

The electron-donating (ω^-) and electron-accepting (ω^+) powers were defined as [47]:

$$\omega^- = \frac{(3I + A)^2}{16(I - A)} \approx \frac{(3\varepsilon_H + \varepsilon_L)^2}{16\eta_K} = \omega_K^-,$$

$$\omega^+ = \frac{(I + 3A)^2}{16(I - A)} \approx \frac{(\varepsilon_H + 3\varepsilon_L)^2}{16\eta_K} = \omega_K^+.$$

Based on these relations, a large ω^+ value corresponds to a better capability of charge accepting, whereas a small
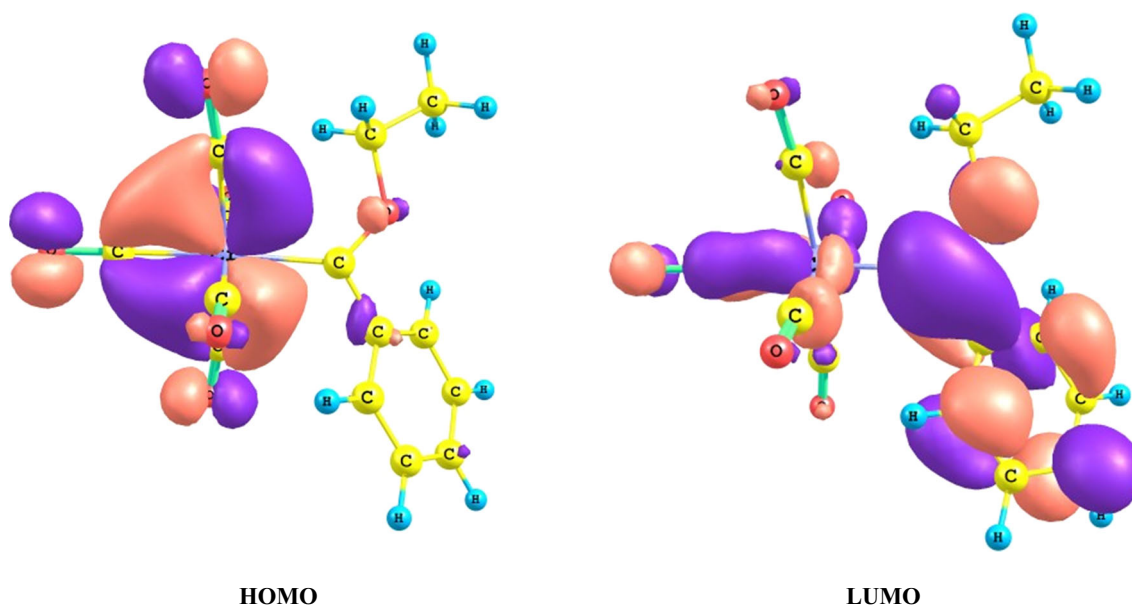
Fig. 3 Frontier orbital plots for [(OC)$_5$Cr=C(OEt)-*para*-C$_6$H$_5$] complex

Table 3 The percentage composition in terms of the defined groups of frontier orbitals for [(OC)$_5$Cr=C(OEt)-*para*-C$_6$H$_4$X] complexes

X	HOMO		LUMO	
	Cr(CO)$_5$	C(OEt)(Ar)	Cr(CO)$_5$	C(OEt)(Ar)
OH	96	4	13	87
NH$_2$	93	7	12	88
Me	96	4	14	86
H	96	4	15	85
Cl	96	4	15	85
CHO	96	4	11	89
COOH	96	4	13	87
CN	96	4	14	86
NO$_2$	96	4	9	91

value of ω^- shows the capability to electron donating. To compare ω^+ with $-\omega^-$, the following definition of net electrophilicity was proposed [48]:

$$\Delta w^{\pm} = w^+ - (-w^-) = w^+ + w^- \approx w_K^+ - (-w_K^-)$$
$$= w_K^+ + w_K^- + \Delta w_K^{\pm},$$

where $\Delta\omega^{\pm}$ is the electroaccepting power relative to the electrodonating power. The results show larger ω^+ values in the presence of EWGs. Therefore, the capability of accepting charge increases in the presence of EWGs. Moreover, with the smaller values of ω^- in the presence of EDGs, the system is a better electron donor in the presence of EDGs.

Energy decomposition analysis (EDA)

The Cr=C chemical bond in these complexes can be regarded as a donor–acceptor orbital interaction, which is schematically illustrated in Fig. 4. The fragments [C(OEt)-*para*-C$_6$H$_4$X] have a doubly occupied σ-orbital, which behaves as a donor orbital, and the empty $p(\pi)$ orbitals behave as acceptor orbitals.

We consider the Cr-C bonding situation in the complexes, which was analyzed with the EDA using the [(OC)$_5$Cr] and [C(OEt)-*para*-C$_6$H$_4$X] fragments. The results of EDA reveal that the interaction energies in the studied complexes are − 210.58 to − 204.97 kJ/mol (Table 1). In the (OC)$_5$Cr=C(OEt)(C$_6$H$_5$) complex, the total interaction energy between [Cr(CO)$_5$] and [C(OEt)(C$_6$H$_5$)] is − 208.32 kJ/mol, where the polarization energy of − 239.49 kJ/mol stabilized the adduct while the sum of the electrostatic and exchange energy destabilized the adduct by 30.38 kJ/mol. For the sake of convenience, it is customary to combine these two terms as a steric term (E_{steric}).

The interaction energy values reveal a stronger interaction between [(OC)$_5$Cr] and [C(OEt)-*para*-C$_6$H$_4$X] fragments in the presence of EDGs.

On the other hand, the magnitude of ΔE_{polar} increases in the presence of EDGs. There is a good linear relationship between these values and the Hammett constants:

$$\Delta E_{\text{polar}} = -13.88\sigma_{\text{p}} - 237.9 \quad R^2 = 0.9636,$$
$$\Delta E_{\text{polar}} = -8.6511\sigma_{\text{p}}^+ - 239.68 \quad R^2 = 0.9888.$$
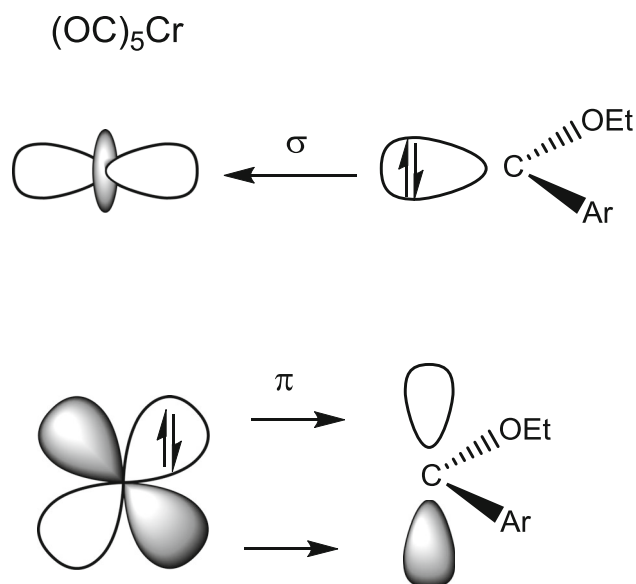
$(OC)_5Cr$

Fig. 4 Schematic representation of the dominant orbital interactions between closed-shell metal fragments [$(OC)_5Cr$] and [$C(OEt)$-*para*-C_6H_4X] ligand fragment (Fischer-type carbene complexes)

Also, the magnitude of E_{steric} increases in the presence of EWGs. There is a good linear relationship between these values and the Hammett constants:

$$E_{\text{steric}} = 16.9\sigma_p + 29.813 \quad R^2 = 0.9919,$$
$$E_{\text{steric}} = 10.924\sigma_p^+ + 32.11 \quad R^2 = 0.9733.$$

Therefore, good correlations can be seen between the ΔE_{polar} and E_{steric} values with Brown's (σ_p^+) compared with the Hammett substituent constants (σ_p).

Topological analyses

Quantum theory of atoms-in-molecules (QTAIM) analysis

It has been proved that the QTAIM-based analysis of electron density can provide valuable information on many physical and chemical properties of molecular systems.

Electron density

The electron density values of Cr=C bonds at corresponding bond critical points (BCP) are listed in Table 4. These data show larger electron density values in the presence of EDGs. The relations between electron density values with Hammett (σ_p) and Brown's (σ_p^+) substituent constants are:

$$\rho = 0.0056\sigma_p + 0.082 \quad R^2 = 0.9526,$$
$$\rho = 0.0037\sigma_p^+ + 0.0828 \quad R^2 = 0.9887.$$

Therefore, there is a good correlation between these electron density values and the Brown's substituent constant compared to the Hammett constant.

A large electron density value corresponds to shorter bonds. The results show shorter bonds in the presence of EDGs. The relation between electron density values and bond distances is:

$$\rho = -0.153r + 0.4055 \quad R^2 = 0.9999.$$

Laplacian of electron density

Laplacian of electron density values of Cr=C bonds ($\nabla^2\rho$) at corresponding BCP is listed in Table 4. These values are positive, likewise those for the closed-shell interactions. Although, the condition $\nabla^2\rho > 0$ and, perhaps, any other measure of charge concentration is not enough to identify chemical bonds [49].

Energy density

The energy density (H) values and its components [Lagrangian kinetic energy (G) and potential energy density (V)] of Cr=C bonds at corresponding BCP are gathered in Table 4. As can be noticed, the energy density values are negative for the shared interactions.

The positive values for Laplacian of electron density and negative values of the energy density of Cr=C bonds at corresponding BCP illustrate that the Cr=C bond has a mix of the closed shell and shared characteristic.

One can also use the ratio $|V(r)|/G(r)$ as another useful description; $|V(r)|/G(r) < 1$ is the characteristic of a typical ionic interaction and $|V(r)|/G(r) > 2$ is defined as a "classical" covalent interaction. Taking all these criteria into consideration, the topological properties at BCP of Cr–C indicate a mixed (partially ionic and partially covalent) character of these coordination bonds because of $1 < |V(r)|/G(r) < 2$ [50].

Interacting quantum atoms (IQA) approach

The mechanism of metal–ligand interactions in the studied complexes was investigated using the atomic energy partitioning method, namely interacting quantum atoms (IQA) [51–54]. This method uses the QTAIM definition of an atom, a nucleus joint with the atomic basin. The overall interaction energy and electrostatic part of the interaction energy for the Cr–C$_{\text{carbene}}$ bond in [$(OC)_5Cr=C(OEt)$-*para*-C₆H₄X] complexes are presented in Table 4. These values reveal that the overall Cr–C$_{\text{carbene}}$ interaction energy, E_{int} (Cr–C$_{\text{carbene}}$), is stabilizing for the studied complexes. The relations between overall interaction energy values with the

Table 4 Electron density (ρ), Laplacian of electron density ($\nabla^2\rho$), the total energy density (H), Lagrangian kinetic energy (G), virial energy density (V), ELF, LOL, the overall interaction energy (E_{int}), and electrostatic part of the interaction energy ($V_{electrostatic}$) for Cr=C bonds of [(OC)$_5$Cr=C(OEt)-*para*-C$_6$H$_4$X] complexes

X	ρ/eÅ^3	$\nabla^2\rho$/eÅ^5	H/a.u.	G/a.u.	V/a.u.	$|V(r)|/G(r)$	ELF	LOL	E_{int}/a.u.	$V_{electrostatic}$/a.u.
OH	0.07961	0.24846	− 0.01742	0.07953	− 0.09695	1.219	0.22045	0.34719	− 0.10860	33.28371
NH$_2$	0.07764	0.23991	− 0.01668	0.07666	− 0.09334	1.218	0.21875	0.34607	− 0.10704	33.11742
Me	0.08184	0.25615	− 0.01835	0.08239	− 0.10075	1.223	0.22416	0.34963	− 0.11230	33.49749
H	0.08295	0.26060	− 0.01880	0.08395	− 0.10276	1.224	0.22545	0.35047	− 0.11366	33.59507
Cl	0.08321	0.26286	− 0.01886	0.08458	− 0.10344	1.223	0.22472	0.34999	− 0.11387	33.62536
CHO	0.08490	0.26905	− 0.01958	0.08685	− 0.10643	1.225	0.22715	0.35157	− 0.11737	33.79519
COOH	0.08463	0.26784	− 0.01948	0.08644	− 0.10591	1.225	0.22697	0.35146	− 0.11589	33.75594
CN	0.08519	0.27115	− 0.01967	0.08745	− 0.10712	1.225	0.22671	0.35129	− 0.11717	33.78486
NO$_2$	0.08587	0.27399	− 0.01995	0.08844	− 0.10839	1.226	0.22740	0.35174	− 0.11749	33.82144

Brown's substituent constant and the Hammett constants are:

$$E_{int} = -0.0076\sigma_p - 0.1126 \quad R^2 = 0.9332,$$
$$E_{int} = -0.0053\sigma_p^+ - 0.1137 \quad R^2 = 0.9957.$$

As can be seen, there is a good correlation between these overall interaction energy values and the Brown's substituent constant compared to the Hammett constant.

ELF analysis

We analyzed the nature of chemical bonding in Cr=C bond on the basis of electron localization function (ELF) distribution, which is indicative of concentrations of valence electron density in regions of chemical bonds.

A large ELF value corresponds to largely localized electrons, suggesting that a covalent bond, a lone pair, or inner shells of the atom are involved. Table 4 reveals larger ELF values in the presence of EWGs. The relation between ELF values and the Hammett constants is:

$$ELF = -0.1693r + 0.5817 \quad R^2 = 0.9696.$$

Moreover, the relations between ELF values with the Hammett (σ_p) and the Brown's (σ_p^+) substituent constants are:

$$ELF = 0.0059\sigma_p + 0.2238 \quad R^2 = 0.8639,$$
$$ELF = 0.0041\sigma_p^+ + 0.2245 \quad R^2 = 0.9592.$$

Therefore, there is a good correlation between ELF values and the Brown's substituent constant compared to the Hammett constant.

LOL analysis

Localized-orbital locator (LOL) is descriptor developed for electron localization. LOL, which gives simple recognizable patterns in classic chemical bonds, has proved useful in interpreting the structures of exotic materials and the classic examples of freshman chemistry texts. LOL focuses on the topological properties of a kinetic energy density. LOL values of Cr=C bond can be interpreted similarly to ELF. Table 4 shows that the LOL values are larger in the presence of EWGs. The relation between LOL values and bond distances is:

$$LOL = -0.1108r + 0.5837 \quad R^2 = 0.9693.$$

Also, the relations between LOL values with Hammett (σ_p) and the Brown's (σ_p^+) substituent constants are:

$$LOL = 0.0039\sigma_p + 0.3494 \quad R^2 = 0.863,$$
$$LOL = 0.0027\sigma_p^+ + 0.3499 \quad R^2 = 0.9594.$$

Therefore, there is a good correlation between LOL values and the Brown's substituent constant compared to the Hammett constant.

Conclusion

The B3LYP*-based quantum mechanical calculations performed in this study on the effect of different substituents on the Cr=C bond in the [(OC)$_5$Cr=C(OEt)-*para*-C$_6$H$_4$X] complexes revealed that:

1. Cr=C bond distances increased in the presence of EDGs.
2. In the basis of the EDA analysis, the polarization energy stabilized the adduct, while the sum of the electrostatic and exchange energy destabilized it.
3. The largest contribution of HOMO and LUMO arises from the Cr(CO)$_5$ fragment and C(OEt)-*para*-C$_6$H$_4$X group, respectively.
4. The calculated overall interaction energy for Cr–C$_{carbene}$ bond was stabilizing for the studied complexes.

5. ELF and LOL values increased in the presence of EWGs.
6. Electron density, ELF, and LOL of the overall interaction energy values for the Cr–C$_{carbene}$ bond in the studied complexes have good correlations with the Brown's substituent constant compared to the Hammett constant.

Computational methods

The Gaussian 09 suite program was used for the calculations [55]. The standard 6-311G(d,p) basis set was applied for the calculations of systems including C, H, and O [56–59]. Calculations related to Cr element were performed using the element standard Def2-TZVPPD basis set [60]. Geometry was optimized using the B3LYP* method with c3=0.15 [61].

The partial population density of states (PDOS) was used to assess the information of molecular orbitals. The spectrum was convoluted using a full width at half maximum (FWHM) of 0.3 eV. These assessments plus the comprehensive analysis of the contributions of atomic orbitals to the molecular orbitals were performed using the GaussSum 3.0 software package [62].

The bonding interactions between the [(OC)$_5$Cr] and [C(OEt)-*para*-C$_6$H$_4$X] fragments were evaluated using the energy decomposition analysis (EDA) in the Multiwfn 3.3.9 software package [63]. The instantaneous interaction energy (ΔE_{int}) between the two fragments was calculated as:

$$\Delta E_{int} = \Delta E_{polar} + \Delta E_{els} + \Delta E_{Ex},$$

where E_{polar} is the electron density polarization term (the induction term) calculated by subtracting E (SCF last) from E (SCF 1st). E_{els} and E_{Ex} are the electrostatic interaction and the exchange repulsion terms, respectively.

The Multiwfn 3.3.9 software package was also used for the topological analysis of electron density [64]. The computations of calculation of interaction energies within the IQA approach were carried out with the AIMAll package [65].

References

1. Taxak N, Patel B, Bharatam PV (2013) Inorg Chem 52:5097
2. Bourissou D, Guerret O, Gabbaï FP, Bertrand G (2000) Chem Rev 100:39
3. Korotkikh NI, Raenko GF, Pekhtereva TM, Shvaika OP, Cowley AH, Jones JN (2006) Russ J Org Chem 42:1822
4. Fischer EO, Kreis G, Kreiter CG, Müller J, Huttner G, Lorenz H (1973) Angew Chem Int Ed 12:564
5. Depooeter CKR (1981) Chem Rev 81:447
6. Wilkinson SG, Stone FGA, Abel EW (1982) Comprehensive organometallic chemistry, vol 8. Pergamon Press, Oxford, p 40
7. Herndon JW (2013) Coord Chem Rev 257:2899
8. Re RED, Hopkins MD (2005) Coord Chem Rev 249:1396
9. Herndon JW (2003) Coord Chem Rev 243:3
10. Mindiola DJ (2006) Acc Chem Res 39:813
11. Cordiner RL, Gugger PA, Hill AF, Willis AC (2009) Organometallics 28:6632
12. Colebatch L, Hill AF, Shang R, Willis AC (2010) Organometallics 29:6482
13. Herndon JW (2014) Coord Chem Rev 272:48
14. Herndon JW (2015) Coord Chem Rev 286:30
15. Ghiasi R (2015) J Theor Comput Chem 14:1550022
16. Ghiasi R, Mokarram EE (2011) Russ J Phys Chem A 875:1174
17. Ghiasi R, Abdolmohammadi S, Moslemizadeh S (2015) J Chin Chem Soc 62:898
18. Ghobadi H, Ghiasi R, Jamehbozorgi S (2017) J Chin Chem Soc 64:522
19. Shamami MK, Ghiasi R, Asli MD (2017) J Chin Chem Soc 64:522
20. Shamami MK, Ghiasi R (2017) J Chin Chem Soc 64:651
21. Sierra MA (2000) Chem Rev 100:3591
22. Meijere AD, Schirmer H, Duetsch M (2000) Angew Chem Int Ed 39:3964
23. Barluenga J, Santamarıa J, Tomas M (2004) Chem Rev 104:2259
24. Gomez-Gallego M, Mancheno MJ, Sierra MA (2005) Acc Chem Res 38:44
25. Sierra MA, Gomez-Gallego M, Martınez-Alvarez R (2007) Chem Eur J 13:736
26. Lage ML, Fernandez I, Mancheno MJ, Sierra MA (2008) Inorg Chem 47:5253
27. Stockmann A, Kurzawa J, Fritz N, Acar N, Schneider S, Daub J, Engl R, Clark T (2002) J Phys Chem A 106:7958
28. Ottonelli M, Piccardo M, Duce D, Thea S, Dellepiane G (2012) J Phys Chem A 116:611
29. Cheng Y-H, Fang Y, Zhao X, Liu L, Guo Q-X (2002) Bull Chem Soc Jpn 75:1715
30. Pichierri F (2017) Theor Chem Acc 136:114
31. Remya GS, Suresh CH (2016) Phys Chem Chem Phys 18:20615
32. Szatylowicz H, Jezuita A, Siodła T, Varaksin KS, Domanski MA, Ejsmont K, Krygowski TM (2017) ACS Omega 2:7163
33. Ghiasi R, Zamani A (2017) J Chin Chem Soc 64:1340
34. Ghiasi R, Pasdar H, Fereidoni S (2016) Russ J Inorg Chem 61:327
35. Ghiasi R, Heydarbeighi A (2016) Russ J Inorg Chem 61:985
36. Ghiasi R, Pasdar H, Irajizadeh F (2015) J Chil Chem Soc 60:2740
37. Peikari A, Ghiasi R, Pasdar H (2015) Russ J Phys Chem A 89:250
38. Ghiasi R, Amini E (2015) J Struct Chem 56:1483
39. Fashami MZ, Ghiasi R (2015) J Struct Chem 56:1474
40. Ghiasi R, Boshak A (2013) J Mex Chem Soc 57:8
41. Pasdar H, Ghiasi R (2009) Main Group Chem 8:143
42. Egorochkin AN, Kuznetsova OV, Khamaletdinova NM, Domratcheva-Lvova LG (2018) Inorg Chim Acta 471:148
43. Anane H, Houssame SE, Guerraze AE, Guermoune A, Boutalib A, Jarid A, Nebot-Gil I, Tomás F (2008) Cent Eur J Chem 6:400
44. Denning DM, Falvey DE (2017) J Org Chem 82:1552
45. Hammett LP (1937) J Am Chem Soc 59:96
46. Hansch C, Leo A, Taft RW (1991) Chem Rev 91:165
47. Gázquez J, Cedillo A, Vela A (2007) J Phys Chem A 11:1966
48. Chattaraj P, Chakraborty A, Giri S (2009) J Phys Chem A 113:10068
49. Cremer D, Kraka E (1984) Croat Chem Acta 57:1259
50. Espinosa E, Alkorta I, Elguero J, Molins E (2002) J Chem Phys 117:5529

51. Blanco M, Pandás AM, Mckee WC (2014) J Comput Chem 35:1499
52. Pendas AM, Blanco MA, Francisco E (2007) J Comput Chem 28:161
53. Blanco MA, Pendas AM, Francisco E (2005) J Chem Theory Comput 1:1096
54. Francisco E, Pendas AM, Blanco MAA (2006) J Chem Theory Comput 2:90
55. Frisch MJ, Trucks GW, Schlegel HB, Scuseria GE, Robb MA, Cheeseman JR, Scalman G, Barone V, Mennucci B, Petersson GA, Nakatsuji H, Caricato M, Li X, Hratchian HP, Izmaylov AF, Bloino J, Zheng G, Sonnenberg JL, Hada M, Ehara M, Toyota K, Fukuda R, Hasegawa J, Ishida M, Nakajima T, Honda Y, Kitao O, Nakai H, Vreven T, Montgomery JA Jr, Peralta JE, Ogliaro F, Bearpark M, Heyd JJ, Brothers E, Kudin KN, Staroverov VN, Kobayashi R, Normand J, Raghavachari K, Rendell A, Burant JC, Iyengar SS, Tomasi J, Cossi M, Rega N, Millam JM, Klene M, Knox JE, Cross JB, Bakken V, Adamo C, Jaramillo J, Gomperts R, Stratmann RE, Yazyev O, Austin AJ, Cammi R, Pomelli C, Ochterski JW, Martin RL, Morokuma K, Zakrzewski VG, Voth GA, Salvador P, Dannenberg JJ, Dapprich S, Daniels AD, Farkas O, Foresman JB, Ortiz JV, Cioslowski J, Fox DJ (2009) Gaussian 09, revision A02. Gaussian Inc, Wallingford
56. Krishnan R, Binkley JS, Seeger R, Pople JA (1980) J Chem Phys 72:650
57. Wachters AJH (1970) J Chem Phys 52:1033
58. Hay PJ (1977) J Chem Phys 66:4377
59. McLean AD, Chandler GS (1980) J Chem Phys 72:5639
60. Rappoport D, Furche F (2010) J Chem Phys 133:134105
61. Parr RG, Yang W (1989) Density-function theory of atoms and molecules. Oxford University Press, Oxford
62. O'Boyle NM, Tenderholt AL, Langner KM (2008) J Comp Chem 29:839
63. Lu T, Chen F (2012) J Mol Gr Model 38:314
64. Lu T, Chen F (2012) J Comp Chem 33:580
65. Keith TA (2013) AIMAll Version 13.11.04. TK Gristmill Software, Overland Park, KS